

In-Situ Loading of Noble Metal Nanoparticles on Hydroxyl-Group-Rich Titania Precursor and Their Catalytic Applications

Liang-Shu Zhong,[†] Jin-Song Hu, Zhi-Min Cui,[†] Li-Jun Wan,* and Wei-Guo Song*

Beijing National Laboratory for Molecular Sciences, Institute of Chemistry, Chinese Academy of Sciences, Beijing 100080, China

Received May 23, 2007. Revised Manuscript Received July 4, 2007

A novel in-situ route was developed to load well-dispersed palladium (Pd) nanoparticles on the surface of hydroxyl-group-rich titania precursor. Pd nanoparticles are formed by in-situ reduction of Pd(II) by Sn(II); the latter is linked to the surface of TiO₂ precursors through inorganic grafting. The initial Pd nanoparticles then serve as seed for subsequent particle growth and allow us to systematically control the amount and size of the Pd nanoparticles by varying the amount of added PdCl₂. The Pd nanoparticles, with no protection from ligands, are well-dispersed on the TiO₂ precursor surface without aggregation even at a high Pd loading of 22.5 wt %. The method is also extended to introduce other noble metal nanoparticles including Au, Ag, Pt, and their bimetallic nanoparticles onto the TiO₂ precursor surface. The as-obtained TiO₂ precursor–Pd composite is a promising catalyst in nanocatalysis. As an example, the TiO₂ precursor–Pd shows high catalytic activity for Suzuki cross-coupling reaction and can be recycled multiple times without loss of activity.

Introduction

Nanocatalysis is essential for chemistry, material science, and nanoscience.^{1–8} Many noble metal nanoparticles have been used as catalysts in various chemical reactions. For facile catalyst recovery and recycle, noble metal nanoparticles are usually deposited onto the surface of solid supports (e.g., polymer, carbon, metal oxides, clays, and zeolites) to form heterogeneous catalysts.^{9,10} In many cases, there is strong synergistic interaction between noble metal nanoparticles and supports, which can greatly enhance the catalytic activity and selectivity.^{11–13} For example, it has been found that highly dispersed gold nanoparticles on various oxides show a remarkable catalysis activity for CO oxidation at low temperature,¹⁴ a property not found in bulk gold. Tradition-

ally, heterogeneous noble metal catalysts are prepared by the impregnation method, during which the support is immersed into an aqueous solution of a noble metal salt, followed by solvent evaporation and metal reduction in hydrogen.¹⁵ Two other popular preparation methods are coprecipitation (CP) and deposition–precipitation (DP),^{16–18} during which noble metal precursor is either coprecipitated with support precursor or directly deposited on the support surface. For the catalysts prepared by the CP or DP method, the size distribution of metal particles and the degree of dispersion on the support are affected by many procedural factors, such as the type of the support, pH value of the solution, and concentrations of the key components.^{19,20} Another approach is to presynthesize colloidal metal nanoparticles and directly load them onto the supports.^{21,22} In order to attach the colloid metal nanoparticles on the support, the surface of the support is usually modified with suitable functional groups (e.g., NH₂ and SH groups) which strongly anchor the colloid nanoparticles.^{23–26} Recently, Liz-Marzan et al. used an electroless metal plating method to deposit

* Corresponding authors. Tel. and Fax: 10-62558934. E-mail: wanlijun@iccas.ac.cn (L.-J.W.), wsong@iccas.ac.cn (W.-G.S.).

[†] Also in the Graduate School of CAS, Beijing, China.

- (1) Anastas, P. T.; Kirchoff, M. M.; Williamson, T. C. *Appl. Catal. A Gen.* **2001**, *221*, 3.
- (2) Schlögl, R.; Abd Hamid, S. B. *Angew. Chem., Int. Ed.* **2004**, *43*, 1628.
- (3) Scire, S.; Minico, S.; Crisafulli, C.; Satriano, C.; Pistone, A. *Appl. Catal. B Environ.* **2003**, *40*, 43.
- (4) Enache, D. I.; Edwards, J. K.; Landon, P.; Solsona-Espriu, B.; Carley, A. F.; Herzing, A. A.; Watanabe, M.; Kiely, C. J.; Knight, D. W.; Hutchings, G. J. *Science* **2006**, *311*, 362.
- (5) Hughes, M. D.; Xu, Y. J.; Jenkins, P.; McMorn, P.; Landon, P.; Enache, D. I.; Carley, A. F.; Attard, G. A.; Hutchings, G. J.; King, F.; Stitt, E. H.; Johnston, P.; Griffin, K.; Kiely, C. J. *Nature* **2005**, *437*, 1132.
- (6) Corma, A.; Serna, P. *Science* **2006**, *313*, 332.
- (7) Hu, J. S.; Ren, L. L.; Guo, Y. G.; Liang, H. P.; Cao, A. M.; Wan, L. J.; Bai, C. L. *Angew. Chem., Int. Ed.* **2005**, *44*, 1269.
- (8) Liang, H. P.; Zhang, H. M.; Hu, J. S.; Guo, Y. G.; Wan, L. J.; Bai, C. L. *Angew. Chem., Int. Ed.* **2004**, *43*, 1540.
- (9) Bell, A. T. *Science* **2003**, *299*, 1688.
- (10) Astruc, D.; Lu, F.; Aranzas, J. R. *Angew. Chem., Int. Ed.* **2005**, *44*, 7852.
- (11) Zhang, F. X.; Chen, J. X.; Zhang, X.; Gao, W. L.; Jin, R. C.; Guan, N. J. *Catal. Today* **2004**, *93–95*, 645.
- (12) Valden, M.; Lai, X.; Goodman, D. W. *Science* **1998**, *281*, 1647.
- (13) Huang, J.; Jiang, T.; Gao, H. X.; Han, B. X.; Liu, Z. M.; Wu, W. Z.; Chang, Y. H.; Zhao, G. Y. *Angew. Chem., Int. Ed.* **2004**, *43*, 1397.

- (14) Daniel, M. C.; Astruc, D. *Chem. Rev.* **2004**, *104*, 293.
- (15) Gates, B. C. *Chem. Rev.* **1995**, *95*, 511.
- (16) Akande, A. J.; Idem, R. O.; Dalai, A. K. *Appl. Catal. A Gen.* **2005**, *287*, 159.
- (17) Kozlov, A. I.; Kozlova, A. P.; Asakura, K.; Matsui, Y.; Kogure, T.; Shido, T.; Iwasawa, Y. *J. Catal.* **2000**, *196*, 56.
- (18) Claus, P.; Bruckner, A.; Mohr, C.; Hofmeister, H. *J. Am. Chem. Soc.* **2006**, *128*, 11430.
- (19) Haruta, M. *Catal. Today* **1997**, *36*, 153.
- (20) Wolf, A.; Schuth, F. *Appl. Catal. A Gen.* **2002**, *226*, 1.
- (21) Comotti, M.; Li, W. C.; Spliethoff, B.; Schuth, F. *J. Am. Chem. Soc.* **2006**, *128*, 917.
- (22) Zheng, N.; Stucky, G. D. *J. Am. Chem. Soc.* **2006**, *128*, 14278.
- (23) Stoeva, S. I.; Huo, F. W.; Lee, J. S.; Mirkin, C. A. *J. Am. Chem. Soc.* **2005**, *127*, 15362.
- (24) Kim, J.; Lee, J. E.; Lee, J.; Jang, Y.; Kim, S. W.; An, K.; Yu, H. H.; Hyeon, T. *Angew. Chem., Int. Ed.* **2006**, *45*, 4789.
- (25) Mandal, S.; Roy, D.; Chaudhari, R. V.; Sastry, M. *Chem. Mater.* **2004**, *16*, 3714.

silver nanoparticles on the surface of colloid silica spheres.^{27,28} For the purpose of better control of metal loading and effective dispersion, it is still very desirable to develop a simple and reliable protocol for immobilizing noble metal nanoparticles on the surface of the supports.

Herein, we report an in-situ method to reduce Pd(II) by Sn(II) and subsequently to deposit highly dispersed palladium (Pd) nanoparticles onto the surface of hydroxyl-group-rich TiO₂ precursor. The well-dispersed Pd nanoparticles are free of protection ligands, and the as-obtained TiO₂ precursor–Pd exhibits high catalytic activity even at room temperature when used as catalyst for Suzuki cross-coupling reaction. In addition, the as-obtained TiO₂ precursor–Pd catalyst is recycled five times and shows excellent stability due to its heterogeneous composite structure. This synthesis route is also a promising strategy for introducing many other transition metals (such as Au, Ag, Pt, and their bimetallic nanoparticles) onto the TiO₂ precursor surface.

Experimental Section

Synthesis of TiO₂ Precursor Spheres. The titania precursor spheres were synthesized according to the reported procedures with minor modifications.²⁹ In a typical procedure, 2 mL tetrabutoxytitanium (Beijing Chemicals Co.) was added to 50 mL ethylene glycol (Beijing Chemicals Co.) and was magnetically stirred for 8 h at room temperature; then, the mixture was poured into a solution containing 170 mL acetone (Beijing Chemicals Co.) and 2.7 mL water and was vigorously stirred for 1 h. The white precipitate was harvested by centrifugation, followed by washing with ethanol five times and drying at 60 °C for further use.

Loading Pd Nanoparticles onto the TiO₂ Precursor Surface.³⁰ For the synthesis of TiO₂ precursor–Pd with 11.2 wt % Pd loading, 0.1 g TiO₂ precursor sphere powder was added to 20 mL distilled water and stirred for 10 min as part A. 0.1 g SnCl₂ (Beijing Chemicals Co.) was dissolved in 20 mL 0.02 M HCl solution as part B. Parts A and B were mixed together under stirring, and the color of the colloid turned yellow quickly. Ten min later, the precipitate was recovered by centrifugation, followed by washing with distilled water five times, and was dispersed into 40 mL distilled water, resulting in a milky yellow colloidal mixture. Then, 2.5 mL of 0.042 M PdCl₂ (Beijing Chemicals Co.) solution was added to the above mixture and the color turned to blue-black immediately. Five min later, 10 mL of 0.15 M sodium formate (Beijing Chemicals Co.) solution was added. After stirring for 5 h, the black precipitate was recovered by centrifugation and washing with distilled water five times. The precipitate for further characterizations was dried at 60 °C for 12 h. The preparation procedure of TiO₂ precursor–Pd with different Pd loading was the same except that the amount of the added PdCl₂ solution varied.

Suzuki Cross-Coupling Reactions. 10 mg TiO₂ precursor–Pd with 11.2 wt % Pd loading, 1 mmol iodobenzene (Alfa Aesar), 2 mmol phenylboronic acid (Alfa Aesar), 4 mmol K₃PO₄ (Sigma), and 1 mmol pentamethylbenzene (Alfa Aesar, as internal standard for GC analysis) were added to 15 mL ethanol under stirring. After

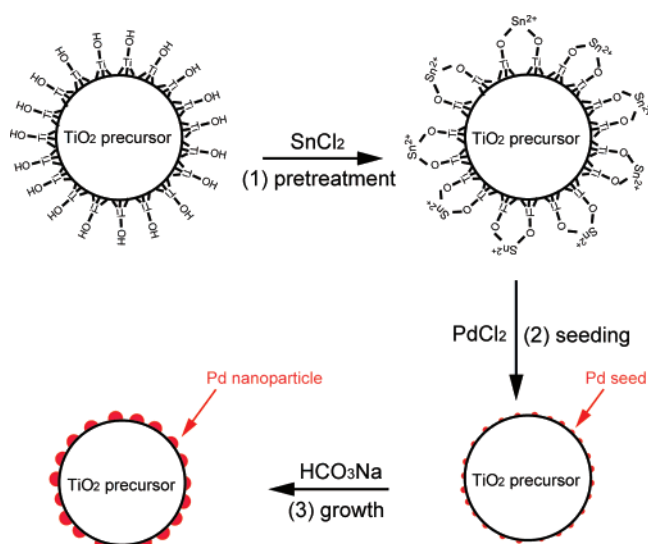


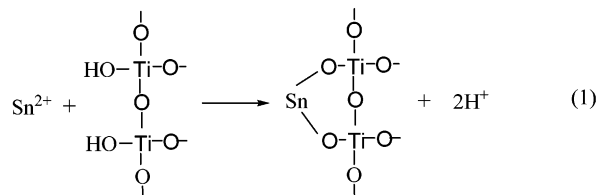
Figure 1. Schematic process for loading Pd nanoparticles onto the surface of TiO₂ precursor. (1) Pretreatment with SnCl₂. (2) In-situ reduction and the formation of Pd nanoparticle seeds. (3) Further growth of Pd nanoparticles.

reflux for 30 min (ca. 78 °C), the solid and liquid were separated by centrifugation and the liquid was analyzed by an Agilent 6890 GC equipped with a flame ionization detector (FID) and a 50 m capillary column. A time-dependent experiment at room temperature using catalysts with different Pd loadings was carried out in the same manner as the above experiment, except that a double amount of Pd catalyst was adopted. A certain amount of the reaction mixture was collected at specific times during the reaction. The solid and liquid was then separated quickly by centrifugation, and the liquid was analyzed by GC.

Characterization. The samples were characterized by scanning electron microscopy (SEM; Hitachi S-4300F), tunneling electron microscopy (TEM; JEM JEOL 2010, with an energy dispersive X-ray (EDX) system), Fourier transform infrared (FTIR; Bruker Tensor 27), and X-ray photoelectron spectroscopy (XPS; VG ESCALAB 220i-XL). Inductively coupled plasma mass spectrometry (ICP-MS; Thermo Electron X II) was adopted to measure the Pd content.

Results and Discussion

Figure 1 schematically depicts the overall preparation procedure for loading Pd nanoparticles onto the surface of hydroxyl-group-rich TiO₂ precursor. The method is essentially a three-step process. The first step is to link the Sn(II) to the TiO₂ precursor surface through inorganic grafting by the following reaction (eq 1).^{31,32}



This linkage is achieved by impregnating TiO₂ precursor into SnCl₂ solution and attaching the Sn(II) onto the TiO₂

(26) Hanaoka, T.; Kormann, H. P.; Kroll, M.; Sawitowski, T.; Schmid, G. *Eur. J. Inorg. Chem.* **1998**, 807.

(27) Kobayashi, Y.; Salgueirino-Maceira, V.; Liz-Marzan, L. M. *Chem. Mater.* **2001**, *13*, 1630.

(28) Schierhorn, M.; Liz-Marzan, L. M. *Nano Lett.* **2002**, *2*, 13.

(29) Jiang, X. C.; Herricks, T.; Xia, Y. N. *Adv. Mater.* **2003**, *15*, 1205.

(30) Zhong, L. S.; Hu, J. S.; Wan, L. J. A method for loading noble metal nanoparticles to solid surface and its applications. Chinese Patent 200710063046.8, 2007.

(31) Lakshmi, B. B.; Patrissi, C. J.; Martin, C. R. *Chem. Mater.* **1997**, *9*, 2544.

(32) Kennedy, J. F.; Cabral, J. M. S. *Solid Phase Biochemistry*; Wiley: New York, 1983; Vol. 66.

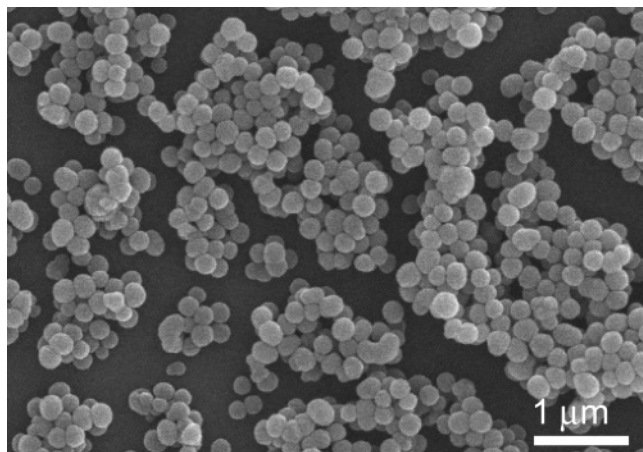


Figure 2. SEM image of the TiO₂ precursor spheres used for loading Pd nanoparticles.

precursor surface. In the second step, the linked Sn(II) species acts as a reducing reagent to reduce Pd(II) in-situ. The

standard reduction potential of the Pd²⁺/Pd redox pair (0.951 V vs the standard hydrogen electrode (SHE)) is higher than that of Sn⁴⁺/Sn²⁺ (0.151 V vs SHE);³³ thus, the reduction of Pd(II) is facile. The third step is controlled growth of Pd around the initial Pd clusters to form nanoparticles. First, the TiO₂ precursor spheres (made of mostly titanium glycolate) are synthesized according to the reported procedure with minor modifications²⁹ and taken as an example of a substrate with a rich hydroxyl group to load with metal nanoparticles. The scanning electron microscopy image of the as-prepared TiO₂ precursor (Figure 2) shows nearly monodispersed spheres (ca. 200 nm in diameter). Fourier transform infrared (FTIR) spectra (Figure S1 in the Supporting Information) shows that the peaks corresponding to the hydroxyl group (the O–H stretching band at around 3380 cm⁻¹ and the O–H bending mode at around 1645 cm⁻¹) are rather strong, indicating abundant hydroxyl groups. Figure 3 depicts the TEM images of the samples during different

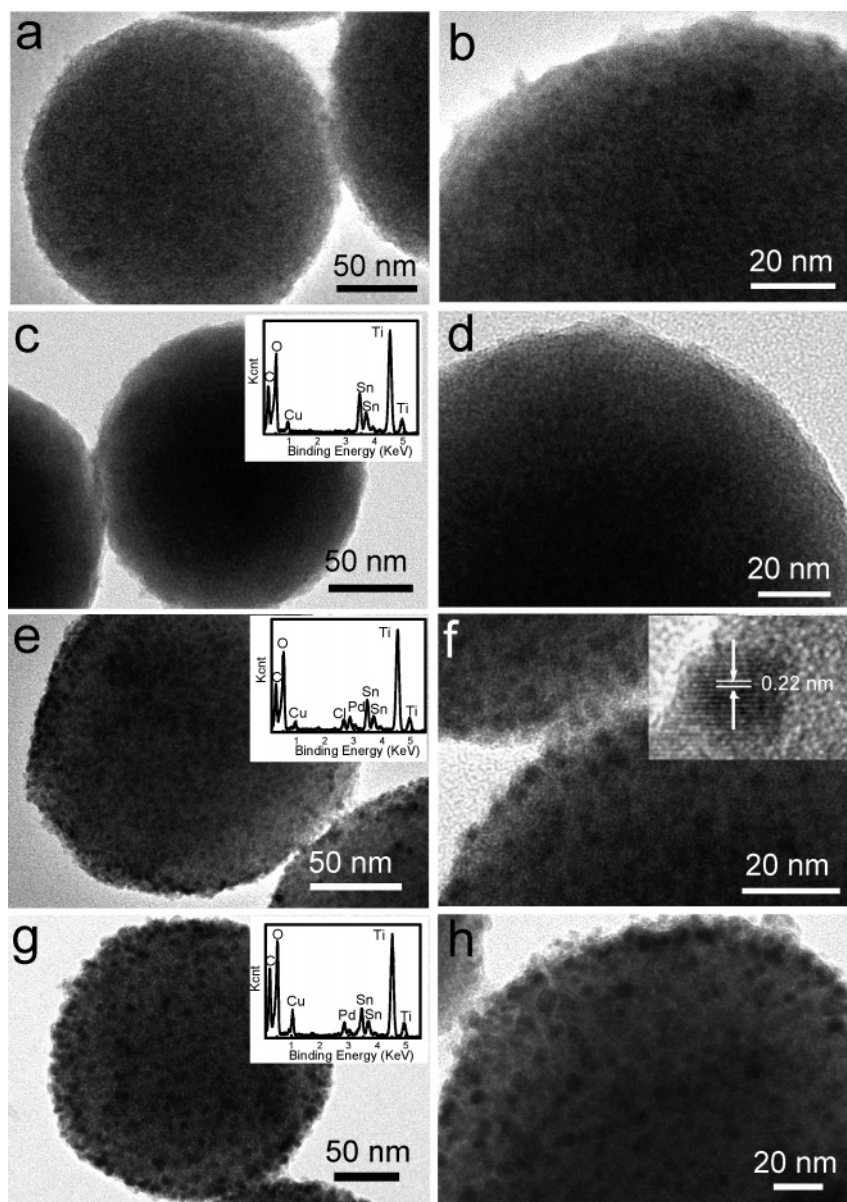


Figure 3. TEM images of the samples during different preparation stages with low (left) and high (right) magnification: (a and b) TiO₂ precursor; (c and d) TiO₂ precursor after the pretreatment with SnCl₂; (e and f) TiO₂ precursor with the Pd clusters before growth (the inset of f is the HRTEM image); (g and h) TiO₂ precursor with Pd nanoparticles after growth (11.2 wt % Pd loading). The insets of c, e, and g are the EDX analyses of the corresponding samples, respectively.

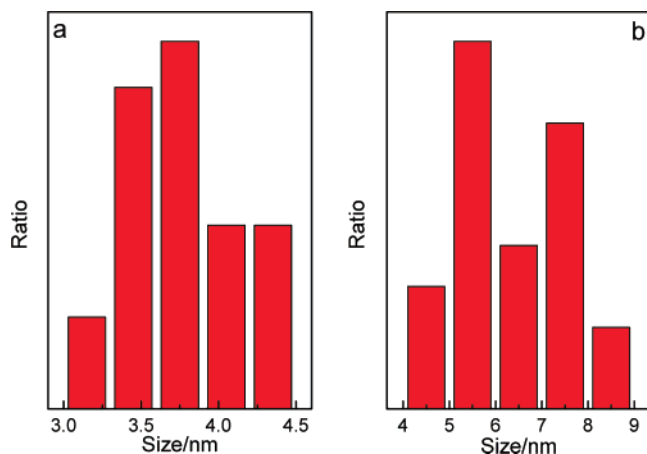


Figure 4. Size distribution of Pd nanoparticles. The nanoparticles are shown before (a) and after (b) growth on the surface of the TiO₂ precursor (11.2 wt % Pd loading).

stages of the procedure. The surface of TiO₂ precursor spheres is rather smooth (Figure 3a and b). Afterward, the TiO₂ precursor spheres are immersed into a SnCl₂ solution to attach Sn(II) to their surface. Ten min later, the excess Sn(II) ions from solution are removed by five consecutive centrifugation/redispersion steps. After such pretreatment with SnCl₂ solution, the surface of TiO₂ precursor spheres remains smooth as shown in Figure 3c and d. Energy-dispersive X-ray (EDX) analysis of the TiO₂ precursor after the pretreatment with SnCl₂ indicates the presence of Sn(II) (inset of Figure 3c). The colloidal Sn(II)-linked TiO₂ precursor is then mixed with a solution of PdCl₂ under stirring. The colloidal solution turned blue-black quickly, indicating that the Pd(II) is reduced by Sn(II) on the surface of the TiO₂ precursor. EDX analysis (inset of Figure 3e) further confirms the existence of Pd. The Sn(II) ions adsorbed on the surface act as reducing agents to ensure that the reduction only takes place on the surface. The resulting Pd atoms by in-situ reduction form small clusters and attach to the surface of the TiO₂ precursor. The previously smooth surface becomes rough (Figure 3e). Figure 3f shows Pd clusters (the small dark spheres) with an average size of 3.8 ± 0.4 nm (Figure 4a) that are uniformly distributed on the surface of the TiO₂ precursor. A representative high-resolution TEM (HRTEM) image taken from the Pd cluster was shown in the inset of Figure 3f. The lattice fringes were clearly visible with a spacing of 0.22 nm, which corresponded to the lattice spacing of the (111) planes of Pd. These Pd clusters can also act as seeds for further particle growth, which is achieved by adding sodium formate solution into the blue-black colloidal solution. With sodium formate, the Pd(II) remaining in the solution is reduced and attached to the previously formed Pd cluster, leading to larger Pd clusters. In the end, all Pd(II) is reduced and deposited on the TiO₂ surface. TEM images of the as-obtained TiO₂ precursor–Pd (11.2 wt % Pd loading) composite are shown in Figure 3g and h. The Pd nanoparticles are remarkably well-dispersed, and no aggregation is observed. The average size of the Pd nanoparticles is increased to 6.4 ± 1.2 nm (Figure 4b). The as-obtained TiO₂ precursor–Pd composite is also investigated by EDX analysis and X-ray photoelectron spectroscopy (XPS). The XPS Pd3d spectra (Figure 5)

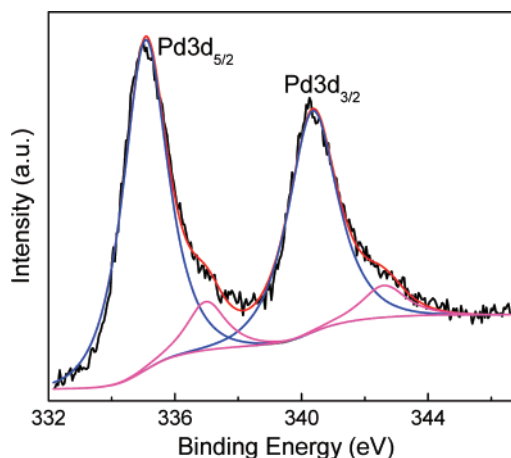


Figure 5. XPS Pd3d pattern of as-obtained TiO₂ precursor–Pd.

verifies the presence of both of metallic palladium and Pd(II) on the sample.³³ The Pd3d signal from metallic palladium is more intensive than that of Pd(II), indicating that most of palladium exists in its metal form.

The content of Pd loading on TiO₂ precursor as well as the size of Pd nanoparticles can be conveniently controlled by varying the amount of the added PdCl₂. When the Pd loading is decreased to 2.2 wt %, the Pd nanoparticles (Figure 6a) are well-dispersed on the TiO₂ precursor surface with a size distribution of 4.0 ± 0.7 nm. When the Pd loading is further decreased to 0.7 wt %, it is hard to distinguish the Pd nanoparticles by TEM, indicating that the size of the Pd nanoparticles is indeed very small. On the other hand, when the Pd loading is increased to 22.5 wt %, many discrete Pd nanoparticles on the surface of TiO₂ spheres can be found (Figure 6b), and the average size of these Pd nanoparticles increases to 8.8 ± 1.0 nm. As shown in Figure 6b, though the Pd loading is rather high (22.5 wt %), the Pd nanoparticles are still well-dispersed and no aggregation occurs.

This synthesis route also applies for loading other transition metal nanoparticles (such as Au, Ag, Pt, and their bimetallic alloy nanoparticles) onto the TiO₂ precursor surface. When AgNO₃ or HAuCl₄ is used instead of PdCl₂, TiO₂ precursor–Ag or TiO₂ precursor–Au is successfully prepared by this method. As shown by Figure 7, the Ag and Au nanoparticles are also well-dispersed on the TiO₂ precursor surface with average sizes of 6.0 ± 0.9 and 5.3 ± 0.8 nm, respectively.

In the present study, when the milky white TiO₂ precursor colloid solution is mixed with SnCl₂ solution, the color of the mixture quickly turns yellow, indicating that the Sn(II) ions have fast interaction with TiO₂ precursor. During this pretreatment stage, the hydroxyl groups on the surface of TiO₂ precursor strongly chelate with Sn(II).^{31,32} Since the surface of TiO₂ precursor is hydroxyl rich, the amount of Sn(II) attached to the surface by chemical linking reaction is plenty. Thus, many Pd nanoparticles can be formed on the TiO₂ precursor surface. In a control experiment, without the pretreatment with SnCl₂, the TiO₂ precursor colloid solution is mixed with PdCl₂ and sodium formate solution overnight. The resulting product is also investigated by TEM

(33) Diaz, R.; Arbiol, J.; Cirera, A.; Sanz, F.; Peiro, F.; Cornet, A.; Morante, J. R. *Chem. Mater.* **2001**, *13*, 4362.

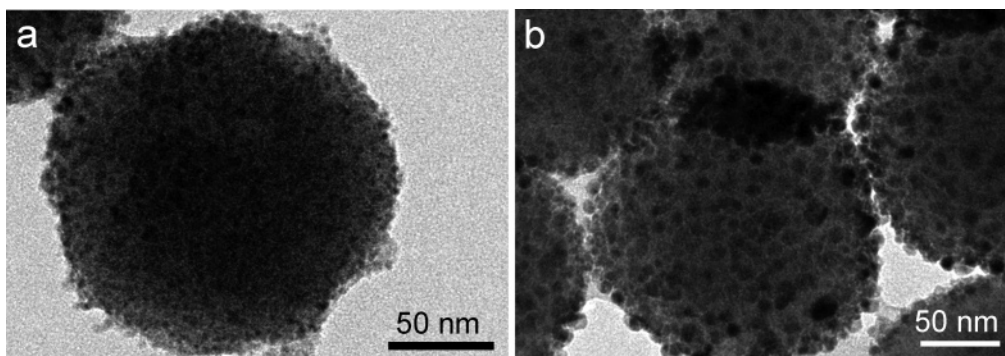


Figure 6. TEM images of the TiO₂ precursor–Pd with different Pd loadings: (a) 2.2 and (b) 22.5 wt %.

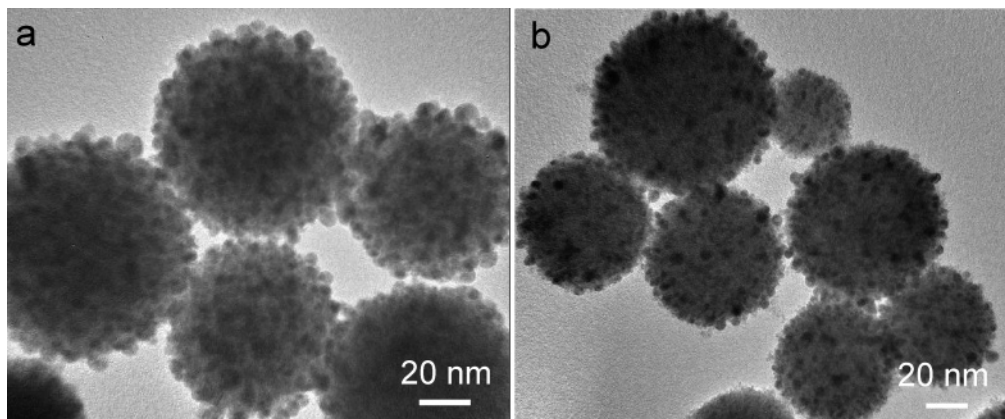


Figure 7. TEM images of the as-prepared TiO₂ precursor–Ag (a) and TiO₂ precursor–Au (b) composites.

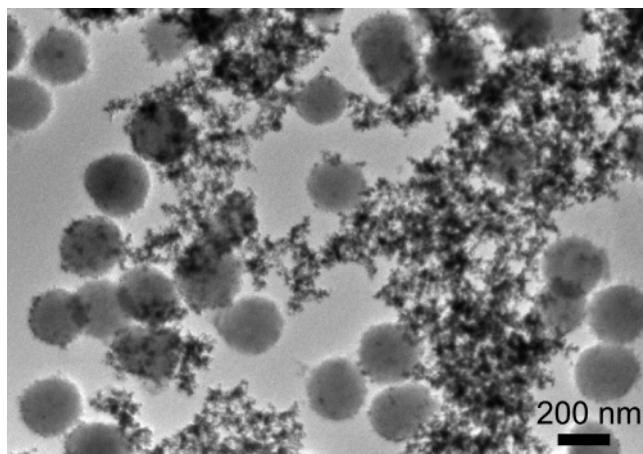
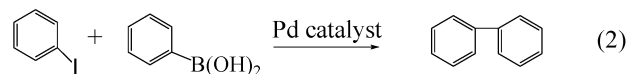


Figure 8. TEM image of the TiO₂ precursor–Pd prepared without the pretreatment with SnCl₂.

(Figure 8), showing that most of the Pd nanoparticles are not deposited onto the TiO₂ precursor surface. This indicates that the pretreatment of TiO₂ precursor with SnCl₂ is vital for the successful loading of Pd nanoparticles onto the surface, as the Sn(II) linkage provides a strong anchor on the TiO₂ precursor surface for initially formed Pd clusters, which in turn provide seeds for further particle growth on the TiO₂ precursor surface. Furthermore, although spherical TiO₂ precursor made of titanium glycolate is selected in present study, it should be noted that other hydroxyl-group-rich TiO₂ precursors with different chemical composition can be used as well. And, the morphology of the TiO₂ precursor has little effect on the loading of noble metal nanoparticles.

As a transition noble metal catalyst, palladium is widely used in various catalytic reactions.^{34–38} The features that make the TiO₂ precursor–Pd catalyst in present study particularly attractive are the following: (1) the surface area of the actual catalyst, Pd particles, is very high as the sizes of the Pd nanoparticles are rather small (several nanometers); (2) the active sites on Pd nanoparticles are not blocked by the protection ligands, inferring high catalytic activity; (3) facile mass transfer is possible as the Pd nanoparticles are well-dispersed onto the TiO₂ surface without aggregation; (4) separation and recycling of the catalyst are also facile due to the heterogeneous composite structure.

The palladium-catalyzed Suzuki cross-coupling reaction of arylboronic acid and aryl halide is an effective synthetic route for biaryls.^{39–42} Herein, Suzuki cross-coupling of iodobenzene and phenylboronic acid is adopted as a model reaction to test the catalytic ability of the TiO₂ precursor–Pd catalyst (eq 2).



The reaction is carried out using TiO₂ precursor–Pd (11.2 wt % Pd loading) catalyst. After 30 min of reaction time the

- (34) Tsuji, J. *Palladium reagents and catalysts, new perspective for the 21st century*; Wiley: Chichester, 2004.
 (35) Kiss, G. *Chem. Rev.* **2001**, *101*, 3435.
 (36) Beletskaya, I. P.; Cheprakov, A. V. *Chem. Rev.* **2000**, *100*, 3009.
 (37) Zimmer, R.; Dinesh, C. U.; Nandan, E.; Khan, F. A. *Chem. Rev.* **2000**, *100*, 3067.
 (38) Drent, E.; Budzelaar, P. H. M. *Chem. Rev.* **1996**, *96*, 663.
 (39) Cho, J. K.; Najman, R.; Dean, T. W.; Ichihara, O.; Muller, C.; Bradley, M. J. *Am. Chem. Soc.* **2006**, *128*, 6276.
 (40) Miyaura, N.; Suzuki, A. *Chem. Rev.* **1995**, *95*, 2457.

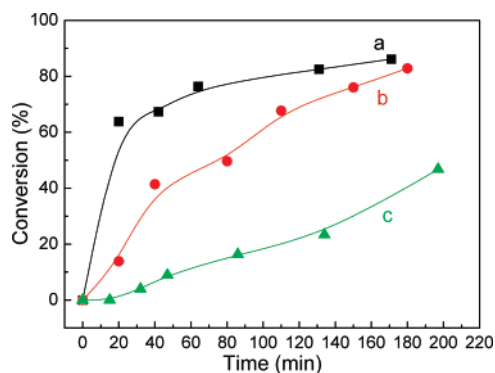


Figure 9. Activity profiles for the Suzuki coupling reaction by the TiO_2 precursor-Pd samples with different Pd loadings at room temperature: (a) 2.2; (b) 11.2; and (c) 22.5 wt %.

conversion reaches 100% with 99% yield, indicating that the TiO_2 precursor-Pd catalyst is quite active for this reaction. This catalytic activity is much higher than that of the hollow palladium spheres under similar reaction condition, where more than 2 times the amount of Pd catalyst and 6 times the reaction time are needed to achieve similar conversion.⁴³ The TiO_2 precursor-Pd is also active for the Suzuki coupling reaction between bromobenzene and phenylboronic acid and for the Mizoroki-Heck coupling reaction.

The TiO_2 precursor-Pd can be recycled up to five times without apparent loss of activity. The conversion is above 95% in all five rounds of recycling. Recently, Hyeon et al. reported that the yield of the catalytic coupling reactions with Pd nanoparticles assembled on silica spheres gradually decreased as recycling proceeded due to the significant loss of Pd nanoparticles.²⁴ The TEM image of the TiO_2 precursor-Pd catalyst after five catalyst recycles (Figure S2 in the Supporting Information) shows that the Pd nanoparticles remain highly dispersed on the surface of the TiO_2 precursor. No detachment or aggregation of Pd nanoparticles during the catalytic reaction is observed. After the catalytic reaction, the supported Pd catalyst was filtered off and the Pd content in the solution was found to be 0.8 ppm based on ICP-MS elemental analysis, indicating that a very small amount of Pd (ca. 1% of the total loading Pd) was possibly leached. This allows the TiO_2 precursor-Pd catalyst to preserve excellent activity during multiple recycles.

In order to investigate the effect of the Pd loading on their catalytic activities, three TiO_2 precursor-Pd catalysts with 2.2, 11.2, and 22.5 wt % Pd loadings were tested for the time-dependent Suzuki coupling reaction. Since the catalytic activities of all three samples were too high at ethanol refluxing temperature, these experiments were carried out at room temperature. After reaction for a specific time, a certain amount of the reaction mixture was collected and analyzed. Figure 9 shows the activity profiles of the three catalysts for Suzuki coupling reaction. For the first hour of reaction time, the TOFs (turn-over frequency) to iodobenzene of the three catalysts are 34.9, 21.8, and 5.4 h^{-1} for the

samples with 2.2, 11.2, and 22.5 wt % Pd loading, respectively. The TiO_2 precursor-Pd with 2.2 wt % Pd loading shows the highest rate while the sample with 22.5 wt % Pd loading shows the lowest rate (the amounts of Pd metal on all three catalysts are kept the same by using a proper amount of the catalysts). As shown in Figure 6, the size of the Pd nanoparticles decreases with the decrease of Pd loading, so that the higher catalytic activity on 2.2 wt % loading catalyst is very likely due to a smaller Pd particle size. This trend was also consistent with the reported study of cluster-size effects in Heck and Suzuki reactions which proposed that catalysis occurred at defect sites on the cluster surface.²⁸

There is debate over whether the reaction is catalyzed by the nanoparticles on the solid surface or by leached Pd species.^{39,44} Recently, Rothenberg et al. proposed that leached Pd species were the true catalyst in the C-C coupling reactions.⁴⁵ In the present study, after separating the solid catalyst by centrifugation, the same amount of reactants were added to the clear solution to repeat the Suzuki reaction without solid catalyst and ca. 30% of iodobenzene was converted after 3 h at room temperature, while the conversion was ca. 75% for the solid catalyst with 11.2 wt % Pd content; so, the contribution from the small amount of leached Pd species might be significant. Further studies are carried on to reveal the true catalysis mechanism.

Conclusion

In conclusion, a novel route is developed to load Pd nanoparticles onto the surface of hydroxyl-group-rich TiO_2 precursor. The method is based on in-situ Pd(II) reduction by Sn(II) species that are linked to the surface of the TiO_2 precursor. The Pd loading and the size of Pd nanoparticles are readily controlled by varying the amount of the added PdCl_2 . The Pd nanoparticles are free of protection ligands and are well-dispersed on the surface without aggregation even at the high loading of 22.5 wt %. The present method is versatile, and many transition noble metals and their bimetallic nanoparticles can be loaded onto the surface of TiO_2 precursor by this in-situ route. When used as catalyst for Suzuki cross-coupling reaction, the as-obtained TiO_2 precursor-Pd catalyst shows high catalytic activity and can be recycled up to five times without any notable loss of catalytic activity.

Acknowledgment. This work was partially supported by the National Natural Science Foundation of China (Nos. 20121301, 20575070, 20603041, 20673121, 20673125, and 20520140277), the National Key Project on Basic Research (No. 2006CB806100 and 2002CCA03100), and the Chinese Academy of Sciences.

Supporting Information Available: The FTIR spectra of the TiO_2 precursor and TEM image of the used catalyst. This material is available free of charge via the Internet at <http://pubs.acs.org>.

CM0714032

(41) Choudary, B. M.; Madhi, S.; Chowdari, N. S.; Kantam, M. L.; Sreedhar, B. *J. Am. Chem. Soc.* **2002**, *124*, 14127.

(42) Crudden, C. M.; Sateesh, M.; Lewis, R. *J. Am. Chem. Soc.* **2005**, *127*, 10045.

(43) Kim, S. W.; Kim, M.; Lee, W. Y.; Hyeon, T. *J. Am. Chem. Soc.* **2002**, *124*, 7642.

(44) Davies, I. W.; Matty, L.; Hughes, D. L.; Reider, P. J. *J. Am. Chem. Soc.* **2001**, *123*, 10139.

(45) Thathagar, M. B.; ten Elshof, J. E.; Rothenberg, G. *Angew. Chem., Int. Ed.* **2006**, *45*, 2886.